Vol. **110** (2006) *ACTA PHYSICA POLONICA A* No. 5

Proceedings of the 36th Polish Seminar on Positron Annihilation, Turawa, Poland, 2006

Influence of Atomic Sphere Radii on the Electron–Positron Momentum Density Calculated for SiC within the LMTO-ASA

A. Rubaszek*

Institute of Low Temperatures and Structure Research
Polish Academy of Sciences
P.O. Box 1410, 50-950 Wrocław 2, Poland

The atomic sphere approximation consists in replacing the Wigner–Seitz polyhedron, containing individual atom, by the sphere of the same volume. In the case of several not equivalent atoms per primitive cell, e.g. for SiC, the radii of atomic spheres, centred at different atoms, are not uniquely determined and should be judiciously chosen. In the present work one studies the effect of choice of atomic sphere radii on the resulting electron band structure and momentum density as well as the electron–positron momentum density. Calculations were performed for SiC within the linear muffin-tin orbital atomic sphere approximation method.

PACS numbers: 78.70.Bj, 71.15.Ap, 71.20.Mq

1. Introduction

The electronic properties of SiC, Si, and C have been widely studied [1–3]. The increasing interest in these semiconductors is mainly due to their vital importance for industry and technology. Here the positron annihilation spectroscopy is a sensitive method to probe the electronic structure of the material under study [4]. In particular, the angular correlation of annihilation radiation experimental data provide useful information on the electron momentum density (EMD), which is an important characteristics of the electron band structure in solids. However, in the interpretation of experimental and theoretical electron–positron (e–p) momentum densities with respect to the electronic structure of the host material, some deal of caution is necessary. In the present work one investigates, how far the e–p momentum density calculated for SiC is sensitive to the details of the lin-

*e-mail: A.Rubaszek@int.pan.wroc.pl

ear muffin-tin orbital atomic sphere approximation (LMTO-ASA) band structure method [5]. The independent particle model (IPM) seems to be most appropriate for this purpose, since the IPM neglects the e–p correlation effect and therefore allows to avoid additional contamination of the picture.

2. Calculations

The IPM e–p momentum density is given by the formula

$$\rho^{\mathrm{IPM}}(\boldsymbol{p}=\boldsymbol{k}+\boldsymbol{G})=\sum_{\boldsymbol{k}j}\left|\int_{\Omega}\exp(-\mathrm{i}\boldsymbol{p}\cdot\boldsymbol{r})\psi_{\boldsymbol{k}j}(\boldsymbol{r})\psi_{+}(\boldsymbol{r})\mathrm{d}^3\boldsymbol{r}\right|^2. \tag{1a}$$

Here $\boldsymbol{p}$ and $\boldsymbol{k}$ stand for momentum in the extended and reduced zone scheme, respectively, $\boldsymbol{G}$ is the reciprocal lattice vector, $\psi_{\boldsymbol{k}j}$ and ψ_{+} denote the electron and positron wave functions and summation runs over all occupied electron Bloch states $\boldsymbol{k}j$. If the positron is uniformly distributed in the unit cell, i.e. if one assumes that $|\psi_{+}(\boldsymbol{r})|^2=1/\Omega$, where Ω is the volume of a primitive cell, then the IPM formula (1a) reduces to the expression which defines the EMD:

$$\rho^{\mathrm{EMD}}(\boldsymbol{p}=\boldsymbol{k}+\boldsymbol{G})=\sum_{\boldsymbol{k}j}\left|(1/\sqrt{\Omega})\int_{\Omega}\exp(-\mathrm{i}\boldsymbol{p}\cdot\boldsymbol{r})\psi_{\boldsymbol{k}j}(\boldsymbol{r})\mathrm{d}^3\boldsymbol{r}\right|^2. \tag{1b}$$

The calculations of the electron and positron wave functions have been performed for SiC within the LMTO-ASA band structure method [5]. Inside the sphere, containing the atom of type t centred at position $\boldsymbol{q}_t$, the LMTO-ASA wave functions for an electron in the state $\boldsymbol{k}j$ and a positron in its ground state $\boldsymbol{0}1$ are approximated in the form

$$\psi_{\boldsymbol{k}j}(\boldsymbol{r})=\sum_{lm}\mathrm{i}^l Y_{lm}((\boldsymbol{r}-\boldsymbol{q})/|\boldsymbol{r}-\boldsymbol{q}|)\;A^{\boldsymbol{k}j}_{lmt}\varphi^t_l(|\boldsymbol{r}-\boldsymbol{q}|),\quad |\boldsymbol{r}-\boldsymbol{q}_t|\le S_t, \tag{2a}$$

$$\psi_{+}(\boldsymbol{r})=B^{\boldsymbol{0}1}_t\varphi^t_{+}(|\boldsymbol{r}-\boldsymbol{q}|),\quad |\boldsymbol{r}-\boldsymbol{q}_t|\le S_t. \tag{2b}$$

Here $Y_{lm}(\boldsymbol{r}/r)$ are the spherical harmonics, l and m denote the orbital and magnetic quantum numbers, $\varphi^t_l(r)$ and $\varphi^t_{+}(r)$ are the solutions of the radial electron and positron Schrödinger equation inside the sphere of type t and S_t is the radius of the atomic sphere (AS) centred at $\boldsymbol{q}_t$. The radial functions φ^t_l and φ^t_{+} are normalised to unity inside the relevant AS. Subject to the condition that the electron and positron wave functions are normalised to unity in the unit cell, the associated eigenvector coefficients, $A^{\boldsymbol{k}j}_{lmt}$ and $B^{\boldsymbol{0}1}_t$, fulfil the relation $\sum_{lmt}|A^{\boldsymbol{k}j}_{lmt}|^2=\sum_t|B^{\boldsymbol{0}1}_t|^2=1$.

The corresponding EMD and IPM e–p momentum density read as

$$\rho^{\mathrm{EMD}}(\boldsymbol{p}=\boldsymbol{k}+\boldsymbol{G})=\sum_{\boldsymbol{k}j}\left|(1/\sqrt{\Omega})\sum_{Lt}\exp(-\mathrm{i}\boldsymbol{p}\cdot\boldsymbol{q})\mathrm{i}^l Y_L(\boldsymbol{k}/k)A^{\boldsymbol{k}j}_{Lt}\right.$$
$$\left.\times\int_0^{S_t} j_l(pr)\phi^t_l(r)r^2\mathrm{d}r\right|^2 \tag{3a}$$

and

$$\rho^{\mathrm{IPM}}(\boldsymbol{p}=\boldsymbol{k}+\boldsymbol{G}) = \sum_{\boldsymbol{k}j} |\sum_{Lt} \exp(-\mathrm{i}\boldsymbol{p}\cdot\boldsymbol{q})\mathrm{i}^l Y_L(\boldsymbol{k}/k) A_{Lt}^{\boldsymbol{k}j} B_t^{\mathbf{01}}$$
$$\times \int_0^{S_t} j_l(pr)\phi_l^t(r)\varphi_+^t(r)r^2\mathrm{d}r|^2, \tag{3b}$$

where $L = (l, m)$ and $j_l(x)$ are the spherical Bessel functions of order l. The Jarlborg–Singh correction [6], taking into account the lack of orthogonality of plane waves inside the AS, was incorporated in terms (3a) and (3b).

The open diamond structure $3C$ was considered. This structure is usually modelled as the fcc lattice, containing four atoms per unit cell. For SiC the two "full" atoms, Si and C, are located at positions $\boldsymbol{q}_1 = (0,0,0)$ and $\boldsymbol{q}_2 = (a/4, a/4, a/4)$, respectively, and two "empty" atoms are at positions $\boldsymbol{q}_3 = (0,0,a/2)$ and $\boldsymbol{q}_4 = (a/4, a/4, 3a/4)$, where a is the lattice constant. In this case the average radii of a sphere containing one atom, S_{av}, is defined in terms of a as

$$\frac{4}{3}\pi S_{\mathrm{av}}^3 = a^3/16.$$

In order to conserve the volume of the primitive cell by the sum of the spheres, the radii of individual AS, centred at Si, C and "empty" atoms, S_{Si}, S_{C}, and S_{empty} respectively, have to fulfil the condition

$$S_{\mathrm{Si}}^3 + S_{\mathrm{C}}^3 + 2S_{\mathrm{empty}}^3 = 4S_{\mathrm{av}}^3.$$

TABLE I

Lattice constants used in the calculations and corresponding average AS radii.

	Si	SiC	C
lattice	5.43 Å ≈	4.35 Å ≈	3.58 Å ≈
constant	10.26 a.u.	8.22 a.u.	6.77 a.u.
S_{av}[a.u.]	2.527	2.024	1.666

The experimental lattice constants for SiC, Si, and C and corresponding values of S_{av} are listed in Table I. It is worth noting that the lattice constant and associated average atomic radius for SiC are intermediate between corresponding values for C and Si. This fact suggests that the AS radii for inequivalent atoms may differ. In the present work three various models were considered:

- *Equal AS*: $S_{\mathrm{Si}} = S_{\mathrm{C}} = S_{\mathrm{empty}} = S_{\mathrm{av}}$.
- *Model* 1: $S_{\mathrm{C}}/S_{\mathrm{Si}} = a_{\mathrm{C}}/a_{\mathrm{Si}}$, $S_{\mathrm{empty}} = S_{\mathrm{Si}}$.
- *Model* 2: $S_{\mathrm{C}}/S_{\mathrm{Si}} = a_{\mathrm{C}}/a_{\mathrm{Si}}$, $S_{\mathrm{empty}} = S_{\mathrm{av}}$.

Here a_{C} and a_{Si} are the experimental lattice constants in carbon and silicon,

TABLE II

Radii of AS centred at individual atoms for three models under study.

	S_{C} [a.u.]	S_{Si} [a.u.]	S_{empty} [a.u.]
equal AS	2.024	2.024	2.024
model 1	1.731	2.134	2.134
model 2	1.546	2.344	2.024

respectively. The resulting atomic radii are given in Table II. It should be noted here that passing from the model of equal AS through model 1 to model 2, one increases the value of S_{Si} and decreases the value of S_{C}.

3. Results and discussion

The change of model causes redistribution of the electronic charge in particular spheres, $n^t(\boldsymbol{r})$. The values of total electron charge contained in individual spheres are listed in Table III. For each of three models under study, the Si sphere is positively charged, while empty spheres have negative charge and contain about one valence electron each. The change in ionicity of the sphere is clearly observed for the C atom: from negative (about $0.4e$) charge for the model of equal volume of AS to positive charge for models 1 and 2. The electrons are shifted from the carbon sphere towards the silicon sphere. Also the change of the radial distribution $n^t(\boldsymbol{r})$ is most pronounced at the carbon atom. Within models 1 and 2, the valence electrons, found close to the boundary of sphere containing the carbon atom, are shifted partially towards the core region of C sphere, and mostly to the interstitial region of the sphere centred at the silicon atom. The differences between the models under study are hardly observed in the core electron distributions.

TABLE III

The total electron and positron charge contained in the individual ASs [a.u.].

	Si		C		empty	
	e^-	e^+	e^-	e^+	e^-	e^+
equal AS	11.996	0.1084	6.386	0.1442	1.618	0.7474
model 1	12.363	0.1297	5.564	0.0677	2.174	0.8026
model 2	13.234	0.2301	4.936	0.0393	1.830	0.7306

The negative charge of empty spheres attracts the positron and the major part of the positron distribution (73–80% depending on the model) is found in this region (see Table III). As concerns the C and Si spheres, positron density distribution follows the changes in the electron charge. The probability of finding a positron in Si sphere is an increasing function of S_{Si} parameter and resulting

valence electron density. The positron charge is shifted from the C sphere as value of S_C and the total electron charge inside the sphere decreases.

The band structures for SiC, calculated within three models, are compared in Fig. 1 for momenta along main crystallographic directions. The slope of the first band is very similar for all the models under study. The 1st band obtained within the model 2 is shifted about 0.1 Ry below its counterpart of the model of equal AS radii. The differences between the models are more pronounced in the shape of the second, third, and fourth bands.

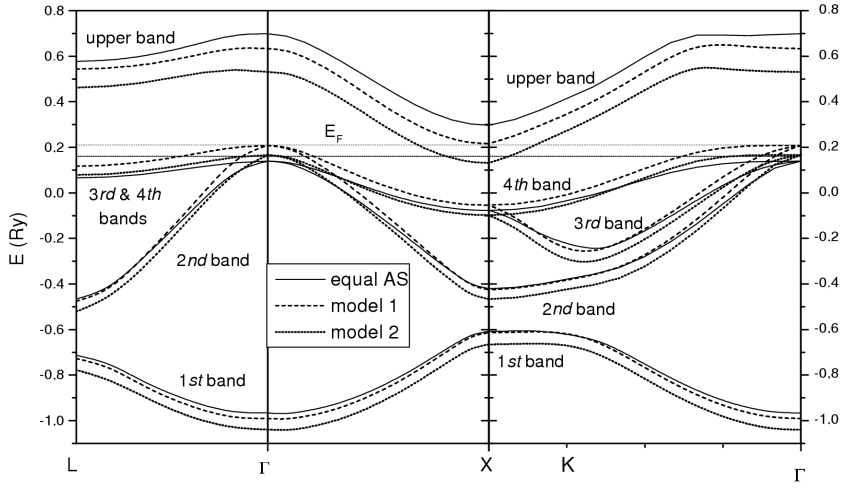

Fig. 1. The band structure calculated for SiC along main crystallographic directions within three various models.

The value of the energy gap, resulting from the model of equal AS radii, amounts to 2.13 eV and is a bit lower than the experimental one, equal to 2.36 eV [1]. It should be noted here that the energy gap, obtained for the model of equal AS radii is strongly diminished to 0.1 eV for the model 1. However, the most striking is the fact that within the model 2 the fifth, upper band starts to contribute to the density of states, energy gap vanishes at all, and the Fermi surface elements appear close to the X point. The latter is in contradiction to well known semiconductor properties of SiC [1].

The band structure details are well reflected in the shape of the electron and electron–positron momentum densities. The slope of these quantities is presented in Fig. 2 for momenta along the direction [100] inside the first and second Jones zone (JZ). Due to the symmetry rules [7], only the 1st and eventually upper (5th) band can contribute to the electron and e–p momentum densities for momenta along the [100] direction inside the first JZ. The contribution of the first band to the EMD is very similar for all three models, as could be expected from the character of this band, discussed previously. For momenta inside the first JZ the effect of

choice of the AS radii model on the resulting spectra is much more pronounced in the e–p momentum density than in the EMD. The same concerns the Fermi surface elements, observed for the model 2. This feature can be attributed to the positron redistribution among individual spheres, which is closely associated with the relevant tendency in the electron charge. In the consequence, the changes in $\psi_{\boldsymbol{k}j}(\boldsymbol{r})$ and $n^t(\boldsymbol{r})$ inside the spheres are considerably enhanced in the overlap terms (3b) by the corresponding changes of $\psi_+(\boldsymbol{r})$.

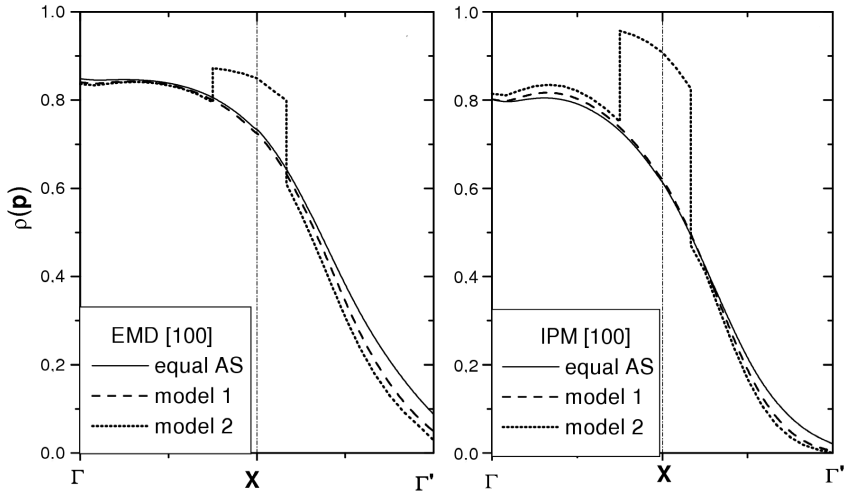

Fig. 2. Electron (left part) and electron–positron (right part) momentum densities in SiC calculated within three models for momenta along [100] direction.

Close to the X point the fifth upper band starts to contribute to the momentum density calculated within the model 2. The non-physical Fermi surface breaks, observed in the EMD spectrum are considerably enhanced by a positron distribution effect, as can be seen in the e–p momentum density slope.

For momenta along the [100] direction inside the second JZ, the only non-zero terms in expressions (1) and (3) may come from the 2nd and upper bands [7]. As can be seen in Fig. 2, the differences between the models occur in the second JZ both for the EMD and IPM spectrum. It should be noted here that the high momentum component of the IPM corresponds to the region, which is probed by a positron with low probability. For this reason the IPM e–p momentum density is diminished as compared to its EMD counterpart, while differences between the models are of comparative order for IPM and EMD.

4. Conclusions

The present study is limited to the EMD and IPM, since these spectra contain *pure* information on the electron and positron distributions in the material

investigated. The e–p correlation effects enhance the picture, presented in the right part of Fig. 2, especially close to the X point.

Concerning the influence of various AS models on the resulting band structure in SiC, one should note here that the LMTO band structure method bases on the density functional theory (DFT) [8]. The principle of the DFT is to find the electron density, which minimizes the total energy of the system. For any model under study this condition is achieved for particular densities n_t. However, the total energy is lower for the model of equal AS radii than for models 1 and 2. The second criterion, due to the ASA, is to reduce the overlap of the spheres, at least in the region of high kinetic energy. Here the model of equal spheres volume seems to be most appropriate.

References

[1] For review and references see e.g. http://www.ioffe.rssi.ru/SVA/NSM/Semicond/SiC/bandstr.html.

[2] For review and references see e.g. http://www.ioffe.ru/SVA/NSM/Semicond/Si/bandstr.html.

[3] For review and references see e.g. http://www.ioffe.ru/SVA/NSM/Semicond/Diamond/bandstr.html.

[4] For review see e.g. M.J. Puska, R.M. Nieminen, *Rev. Mod. Phys.* **66**, 841 (1994); R.M. Nieminen, in: *Positron Spectroscopy of Solids*, Eds. A. Dupasquier, A.P. Mills, IOS Press, Amsterdam 1996, p. 443.

[5] O.K. Andersen, *Phys. Rev. B* **12**, 3600 (1975); W.R.L. Lambrecht, O.K. Andersen, *ibid.* **34**, 2439 (1986).

[6] T. Jarlborg, A.K. Singh, *Phys. Rev. B* **36**, 4660 (1987).

[7] P. Harthoorn, P.E. Mijnarends, *J. Phys. F* **8**, 1147 (1978).

[8] P. Hohenberg, W. Kohn, *Phys. Rev.* **136**, B964 (1964); W. Kohn, L.J. Sham, *ibid.* **140**, A133 (1965).